Copyright © 2011 Tech Science Press CMES, vol.73, no.2, pp.103-135, 2011

A Four-Node Reissner-Mindlin Shell with Assumed Displacement Quasi-Conforming Method

Ping Hu[1], Yang Xia[1] and Limin Tang[2]

Abstract: In this paper, an assumed displacement quasi-conforming finite element method with truncated polynomial expansions of in-domain displacements and derived expansions of strains is introduced. Based on the method a four-node quadrilateral flat shell element with complete quadratic polynomials for membrane and bending displacement fields is developed. Numerical tests are carried out for validation of the present element. The results show that the present element preserves all the advantages of the quasi-conforming i.e., explicit stiffness matrix, convenient post processing and free from membrane locking and shear locking. The tests also prove that the present element gives excellent results, especially for the bending moments, and possesses a stable convergence rate.

Keywords: quasi-conforming, assumed displacement, flat-shell, Taylor polynomial expansion.

1 Introduction

Plate and shell elements are widely used in structural analysis of automotive, aerospace and ship building industries. In engineering analysis, a single element which is able to simulate both thin and moderate thick plate and shell structures with reliable result and sufficient precision is needed. Reissner-Mindlin (R-M) theory provides a choice for this demand, but with traditional displacement based finite element method (FEM), Reissner-Mindlin plate and shell elements give improper results which are always too rigid especially when the thickness is decreasing. This problem is called locking, which is known to all [Zienkiewicz, Taylor and Zhu (2005)]. To solve this, reduced integration (RI) and selective reduced integration

[1] School of Automotive Engineering, Faculty of Vehicle Engineering and Mechanics, State Key Laboratory of Structural Analysis for Industrial Equipment, Dalian University of Technology, Dalian 116024, P.R. China, pinghu@dlut.edu.cn

[2] Department of Engineering Mechanics, Dalian University of Technology, Dalian 116024, P.R. China.

(SRI) techniques are advocated [Yang, Saigal, Masud and Kapania (2000)]. However, the numerical stability of these techniques is governed by the LBB condition and only a limited number of elements can satisfy this condition [Tang and Liu (1984)]. Besides the RI and SRI elements are showed to be mesh-sensitive in engineering analysis practice.

An alternate approach to formulate R-M plate and shell elements can be deduced from the quasi-conforming (QC) finite element method, which was introduced by [Tang, Chen and Liu (1980)] as a basic method of element formulation. This method solves the challenging problem of inter-elements conforming and gives a unified treatment of both conforming and nonconforming elements. The QC technique has been used to construct R-M plate and shell elements almost since it was introduced. Compared to RI and SRI techniques, the QC method is more rational and reliable. In 1985, quasi-conforming technique is used by Tang and Liu to develop an R-M plate element [Tang and Liu (1985)]. Unlike RI and SRI techniques, the QC element uses multiple sets of functions to approximate strain fields and a unique cubic function to approximate deflection in plate. A triangular element with nine nodal values is developed and the element gives quite satisfactory results without locking problem and numerical instability.

Shi and Voyiadjis promoted quasi-conforming method in application of R-M plate and shell in papers [Shi and Voyiadjis (1991b); Shi and Voyiadjis (1991a); Shi and Voyiadjis (1993)] and developed a series of 4-node C_0 elements that are still of great importance nowadays. An approximation for the area integral is introduced to satisfy the Kirchhoff assumption for thin plates and to avoid the time consuming numerical integration. Kim and his group improved Shi and Voyiadjis's element by appending the rotational degree of freedom and obtained a 4-node shell element with good performance [Kim, Lomboy and Voyiadjis (2003); Lomboy, Suthasupradit, Kim and Onate (2009)]. They have done a lot of work with the element, especially on the nonlinear formulations based on the QC technique. Looking back to this not so short history from Tang and Liu's work through Shi and Voyiadjis' to work of Kim et al., a conclusion can be made that QC method have been applied nicely in Reissner-Mindlin plate and shell theory.

In this paper, we resume Kim et al.'s work on quasi conforming Reissner-Mindlin shell within the method of assumed displacement quasi-conforming as opposed to the assumed strain. In Shi or Kim's paper they call the quasi-conforming as assumed strain because obviously the functions to approximate strain fields are set in element formulation. These elements work well but we believe that the assumed strain is a presentative method which is not the essential concept of QC and can not give rational guide to element formulation in universal condition. For example, to decide which items should be chosen for strain function is always a problem.

Incomplete high order items are used in assumed strain method, which will affect the accuracy and stability of the element.

With assumed displacement QC method displacement functions as opposed to strains are set to be the coefficient-undetermined polynomial expansions at the first step (Fig. 1). The expansions for strains are generated accordingly through the strain-displacement equation. Lu et al. had built a thin plate element with similar procedures in [Lu and Xu (1989)], and now in this paper we develop the assumed displacement QC as a basic technique. This system is quite efficient and natural and the process of choosing strain functions is improved. The only thing left to consider is finding a more suitable displacement function. When we choose complete rank polynomials for the fields of displacements, the strains will be completely ranked automatically. We believe the assumed displacement QC is more complete in theory, and better elements can be developed.

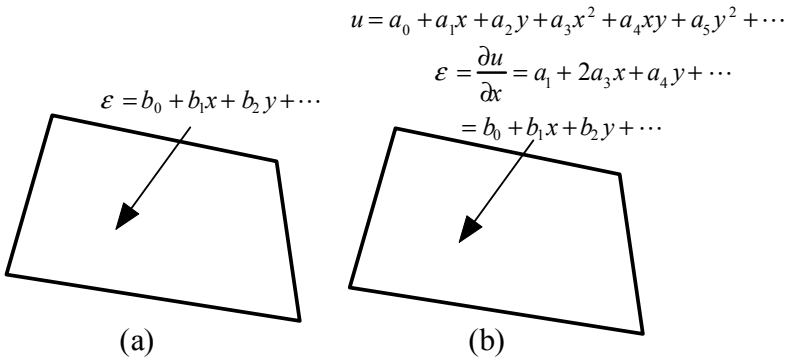

Figure 1: (a) In assumed strain quasi-conforming, the first step in the formulation is the truncated polynomial expansions of the strains; (b) in assumed displacement framework, the first step is expansions of the displacement fields. Polynomial expansions of strains are generated according to the displacements.

Within assumed displacement QC, we formulate a Reissner-Mindlin type plat shell, denoted by QCS1, to obtain an element with a high level of precision and efficiency. The formulation of shell basically follows Shi [Shi and Voyiadjis (1991a)] and Kim [Kim, Lomboy and Voyiadjis (2003)]. For the membrane part, we set the membrane displacements to be complete second rank polynomials, so linear strains can be obtained. The drilling degree of freedom is taken into consideration by applying an Allman type string function and a sub domain assist function. With drilling degrees of freedom, the present element is suitable for analysis of built-up

shell structures [Cai, Paik and Atluri (2010)]. For the bending part, the rotation fields are set to be second rank polynomials; accordingly the bending strains are linear. The membrane and shear strain fields are both completely linear, which is not attained before. Shear strains are set to be constant across the thickness according to linear elastic shell theory. Through explicit fulfillment of Kirchhoff conditions, the element is free from shear locking. The computation method of consistent load is given using the formed in-domain displacement function.

We executed numerous numerical tests to verify the element. The bending patch test is passed and the element can precisely display a pure bending condition. Other standard numerical tests for shell element are carried out and the results show stable and fast convergence rate for both displacement and stress/strain. The stable convergence and accuracy of the stress results are major advantages of our element. The element also performs well under very rough and irregular meshes.

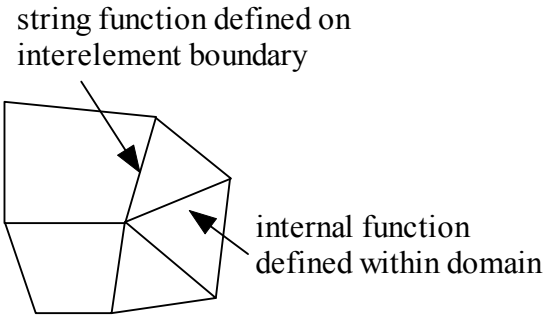

Figure 2: Traditional string function and internal function are still used for discretization. Multiple set of functions are set for an element.

In addition to the benefits derived from the assumed displacement, the advantages of the QC technique are preserved. Traditional string functions and internal functions are still used (Fig. 2). The obtained shell element is guaranteed to provide the convergence result. The stiffness matrix is explicit so the element is efficient compared with elements that require numerical integration.

The paper is organized as follows. In Section 2, the assumed displacement QC finite element method is discussed. In Section 3, we will formulate the shell displacements and strains; finally we get the shell stiffness matrix. Detailed evaluation procedure of strain functions is displayed in Section 4. In Section 5, numerical tests are carried out to verify the element. Finally, results are addressed in Section 6.

2 Paradigm of assumed displacement quasi-conforming

In this section, we will display the paradigm of the assumed displacement QC finite element method. In Subsection 2.1, the major changes are discussed. The first step in QC is Taylor expansion of the displacements as opposed to strains. This simple change will provide a great advantage in favor of the element formulation. Following that in Subsection 2.2 the procedure of element development is displayed, which is similar to assumed strain QC elements. A brief comparison between assumed strain QC elements and assumed displacement QC elements is listed in Tab. 1.

Table 1: Comparison between assumed strain quasi-conforming element and assumed displacement quasi-conforming element

assumed strain quasi-conforming element	**assumed displacement quasi-conforming element**
Formulation starts from strain	Formulation starts from displacement
Flexible strain field assumption	Rational displacements assumption according to Taylor polynomial expansion; strain fields generated from displacements
Domain displacement field not included	Domain displacement field included, conductive to calculation of consistent load and mass matrix
Weak form displacement-strain relationship	
Explicit stiffness matrix	
Guaranteed to get the convergence result	

2.1 First step in assumed displacement quasi-conforming: displacement expansion

In assumed strain formulation, the first step is the truncated Taylor expansion of the strains, and no displacement field is set [Kim, Lomboy and Voyiadjis (2003)]. As a modification we choose the displacement field according to Taylor polynomial expansion first. The strain fields are accordingly obtained by the strain-displacement relations. The displacement fields are

$$\tilde{u} = \begin{Bmatrix} u & v & w & \phi_x & \phi_y \end{Bmatrix} \tag{1}$$

The detailed functions used depend on the problems to be solved. The displacements are assumed to be continuous within the element domain, which are approx-

imated by Taylor's expansion. For the first term u, which is in-plane displacement along x axis, for example, the domain displacement can be set as

$$u = u_0 + (\frac{\partial u}{\partial x})_0 x + (\frac{\partial u}{\partial y})_0 y + \frac{1}{2}(\frac{\partial^2 u}{\partial x^2})_0 x^2 + (\frac{\partial^2 u}{\partial x \partial y})_0 xy + \frac{1}{2}(\frac{\partial^2 u}{\partial y^2})_0 y^2 + \tag{2}$$

Eq. (2) can be expressed by a truncated polynomial expansion,

$$u \approx a_0 + a_1 x + a_2 y + a_3 x^2 + \cdots = \sum_{i=0}^{n} P_i a_i \tag{3}$$

In the above equations, P_i represent the basis trial functions that are chosen from lower order to higher; a_i represent the generalized displacement parameters. The number of terms, denoted by n, is determined by the required precision. The polynomial expansions will converge to Taylor series when the element size diminishes.

The strain fields are set as derivatives of the displacements, so the connections between strain components are taken into fully consideration. For example, the strain $\varepsilon = \frac{\partial u}{\partial x}$ is accordingly set as

$$\varepsilon = \frac{\partial u}{\partial x} \approx a_1 + 2a_3 x + \cdots = \sum_{i=1}^{n} Q_i a_i \tag{4}$$

In the above equations, $Q = \begin{Bmatrix} Q_1 & Q_2 & \end{Bmatrix} = L \begin{Bmatrix} P_1 & P_2 & \end{Bmatrix}$. $L = \frac{\partial}{\partial x}$, which represents the differential operator. The parameter a_0, which means the rigid body displacement, will not appear in the strain function. It can be determined by displacement boundary conditions or other methods introduced in [He and Tang (2002)].

2.2 Forming of element strain-displacement matrix

The above Eq. (4) is weakened within the element domain,

$$\iint_{\Omega} \delta\sigma \left(\frac{\partial u}{\partial x} - \varepsilon \right) dxdy = 0 \tag{5}$$

$\delta\sigma$ is a weighting function, choosing from space which should has the same basis functions to the strain. We set $\delta\sigma$ as Q^T. Substituting (4) into (5),

$$\left[\iint_{\Omega} Q^T Q dxdy \right] a = \iint_{\Omega} Q^T \frac{\partial u}{\partial x} dxdy \tag{6}$$

The formulation can be expressed as

$$Aa = \iint_{\Omega} Q^T \frac{\partial u}{\partial x} dxdy \tag{7}$$

$$A = \iint_{\Omega} Q^T Q dxdy \tag{8}$$

In Eq. (6), the left side is a polynomial function which can be integrated easily. The right side can be calculated with Green's theorem,

$$\iint_{\Omega} Q^T \frac{\partial u}{\partial x} dxdy = \oint_{S} uQ^T n_x dS - \iint_{\Omega} u \frac{\partial Q^T}{\partial x} dxdy \tag{9}$$

S represents the boundary of the element. String net function of displacement u is set along the boundary so the integration can be approximately evaluated.$n_x = \cos(n,x)$ and n means the outside normal direction vector of the boundary. The area integral item in Eq. (9) can be calculated without consideration of the inter element compatibility. We obtain

$$\iint_{\Omega} Q^T \frac{\partial u}{\partial x} dxdy = Cu^e \tag{10}$$

C represents a matrix determined by element node coordinates. u^e represents the displacement parameter of element nodes. Substituting Eq. (10) into Eq. (7), we obtain

$$Aa = Cu^e \tag{11}$$

Finally, the generalized displacement parameter can be expressed by the nodal displacements. The displacement fields and strain fields can be determined.

$$a = A^{-1}Cu^e \tag{12}$$

$$\varepsilon = QA^{-1}Cu^e \tag{13}$$

Eq. (13) can be examined by Taylor expansion, which is analogous to finite difference method. The above scheme called "weak form derivative on boundary" is core concept of QC method, and the concept is versus to weak form in domain derivative of Sobolev space which is formed for equilibrium equations. Detailed description will be given in a forthcoming article with title "Misconception and reform in finite element method" by Tang, L.M., Hu, P. and Xia, Y.

The displacement field can be expressed as,

$$u = a_0 + PA^{-1}Cu^e \tag{14}$$

With the above equations, the finite element formulation can be established.

3 Shell element stiffness formulation

The four-node plat shell element is shown in Fig. 3. The three dimensional shell is represented by the mid-surface. Two sets of coordinate systems are involved, the local coordinate system and the global coordinate system. The origin of the local coordinate is defined to be the geometric center of the element. The stiffness matrix of the single element is calculated in the local coordinate. After a transformation to a global coordinate system, the stiffness matrix is added to the structure stiffness matrix. The definition of a local coordinate system and process of transformation are set according to [Kim, Lomboy and Voyiadjis (2003)]. In this part, we will focus on the element stiffness matrix development. In Subsection 3.1, element stiffness formulations for the membrane part, the bending part and the transverse shear part are given. Then in Subsection 3.2 the combination of these parts to form a complete stiffness matrix is discussed. In Subsection 3.3, we introduce a method to reduce the amount of calculation. In Subsection 3.4, the method to calculate consistent load is displayed.

3.1 Element stiffness formulation

3.1.1 Membrane part

In this part, two in-plane displacement fields $u_m = \begin{Bmatrix} u \\ v \end{Bmatrix}$ are concerned. Subscript "m" represents "membrane".

The functions of displacements are complete linear polynomial expansions, choosing naturally from Taylor polynomial expression.

$$u_m = P_m a_m \tag{15}$$

$$P_m = \begin{bmatrix} 1 & x & y & x^2 & xy & y^2 & 0 & 0 & 0 & 0 & 0 & 0 \\ 0 & 0 & 0 & 0 & 0 & 0 & 1 & x & y & x^2 & xy & y^2 \end{bmatrix} \tag{16}$$

$$a_m = \begin{Bmatrix} a_0 & a_1 & a_2 & a_3 & a_4 & a_5 & b_0 & b_1 & b_2 & b_3 & b_4 & b_5 \end{Bmatrix}^T \tag{17}$$

In the above equations, a_m represents the parameters in polynomials of displacement. Eq. (15) is equally expressed as below for the convenience of notations.

$$u_m = a_{rm} + P_{sm} a_{sm} \tag{18}$$

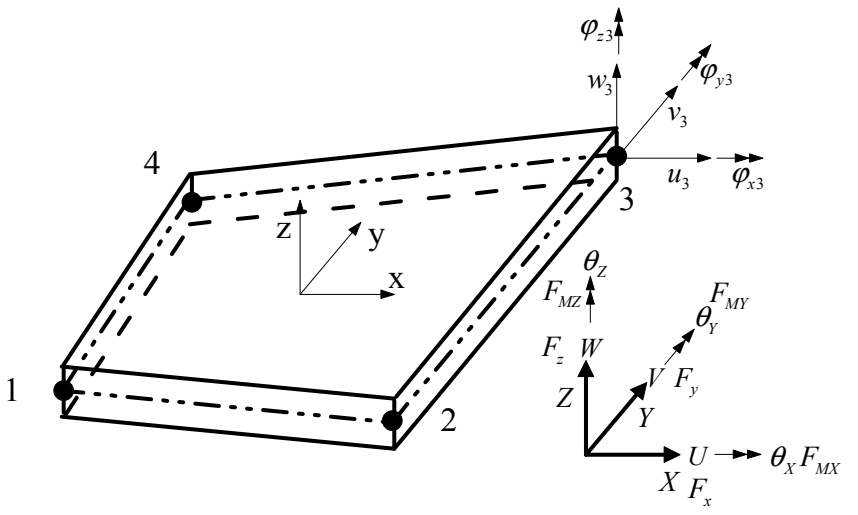

Figure 3: A four node quadrilateral shell element with six degrees of freedom per node

$$a_{rm} = \begin{Bmatrix} a_0 \\ b_0 \end{Bmatrix} \tag{19}$$

$$P_{sm} = \begin{bmatrix} x & y & x^2 & xy & y^2 & 0 & 0 & 0 & 0 & 0 \\ 0 & 0 & 0 & 0 & 0 & x & y & x^2 & xy & y^2 \end{bmatrix} \tag{20}$$

$$a_{sm} = \begin{Bmatrix} a_1 & a_2 & a_3 & a_4 & a_5 & b_1 & b_2 & b_3 & b_4 & b_5 \end{Bmatrix}^T \tag{21}$$

a_{rm} represents parameters for rigid body movements. a_{sm} represents the parameters for movements that generate strains.

The membrane strains are

$$\varepsilon_m = \begin{Bmatrix} \frac{\partial u}{\partial x} & \frac{\partial v}{\partial y} & \frac{\partial u}{\partial y} + \frac{\partial v}{\partial x} \end{Bmatrix}^T = L_m u_m \tag{22}$$

The polynomial expansions of strains are set according to the strain-displacement relation.

$$\varepsilon_m = L_m u_m = L_m P_{sm} a_{sm} = Q_m a_{sm} \tag{23}$$

We choose test functions for membrane strains to be Q_m^T, the weak form of membrane strain is

$$\iint_\Omega Q_m^T Q_m dxdy \cdot a_{sm} = \iint_\Omega Q_m^T \varepsilon_m dxdy \tag{24}$$

In the above equation Ω represents the element domain. The right side is calculated in Part 4.1. Then Eq. (24) is expressed as

$$a_{sm} = A_m^{-1} C_m u_m^e \tag{25}$$

where

$$A_m = \int_\Omega Q_m^T Q_m dxdy \tag{26}$$

$$C_m u_m^e = \iint_\Omega Q_m^T \varepsilon_m dxdy \tag{27}$$

$$u_m^e = \begin{Bmatrix} u_1 & v_1 & \phi_{t1} & \cdots & u_4 & v_4 & \phi_{t4} \end{Bmatrix} \tag{28}$$

u_m^e represents the nodal displacement vector. In membrane part, this vector is comprised of membrane displacements u, v and drilling rotation ϕ_t. Consequently, the membrane strain can be expressed in terms of u_m^e.

$$\varepsilon_m = Q_m a_{sm} = Q_m A_m^{-1} C_m u_m^e = B_m u_m^e \tag{29}$$

With the above equation we can obtain the membrane part stiffness matrix

$$K_m = \iint_\Omega B_m^T D_m B_m dxdy \tag{30}$$

$$D_m = \frac{Eh}{(1-v^2)} \begin{bmatrix} 1 & v & 0 \\ v & 1 & 0 \\ 0 & 0 & \frac{1-v}{2} \end{bmatrix} \tag{31}$$

E, v and h mean Young's modulus, Poisson's ratio and thickness of the shell respectively.

3.1.2 Bending part

The bending of shell element is calculated within the Reissner-Mindlin theory. The formulations are expressed as follows.

$$u_b = \begin{Bmatrix} \phi_x \\ \phi_y \end{Bmatrix} \tag{32}$$

The polynomial expansions of the rotation displacements are chosen to be

$$u_b = P_b a_b = a_{rb} + P_{sb} a_{sb} \tag{33}$$

$$P_b = \begin{bmatrix} 1 & x & y & x^2 & xy & y^2 & 0 & 0 & 0 & 0 & 0 & 0 \\ 0 & 0 & 0 & 0 & 0 & 0 & 1 & x & y & x^2 & xy & y^2 \end{bmatrix} \tag{34}$$

$$P_{sb} = \begin{bmatrix} x & y & x^2 & xy & y^2 & 0 & 0 & 0 & 0 & 0 \\ 0 & 0 & 0 & 0 & 0 & x & y & x^2 & xy & y^2 \end{bmatrix} \tag{35}$$

$$a_{rb} = \begin{Bmatrix} c_0 \\ d_0 \end{Bmatrix} \tag{36}$$

$$a_{sb} = \begin{Bmatrix} c_1 & c_2 & c_3 & c_4 & c_5 & d_1 & d_2 & d_3 & d_4 & d_5 \end{Bmatrix}^T \tag{37}$$

The bending strains are

$$\varepsilon_b = \begin{Bmatrix} \frac{\partial \phi_y}{\partial x} & -\frac{\partial \phi_x}{\partial y} & \frac{\partial \phi_y}{\partial y} - \frac{\partial \phi_x}{\partial x} \end{Bmatrix}^T = L_b u_b \tag{38}$$

According to Eq. (33)

$$\varepsilon_b = L_b u_b = L_b P_{sb} a_{sb} = Q_b a_{sb} \tag{39}$$

The test functions are chosen to be Q_b^T, the weak form of Eq. (39) is

$$\iint_{\Omega} Q_b^T Q_b dxdy \cdot a_{sb} = \iint_{\Omega} Q_b^T \varepsilon_b dxdy \tag{40}$$

Similar to formulations of membrane strain, the bending strain can be expressed by the nodal rotation displacement parameters.

$$\varepsilon_b = Q_b a_{sb} = Q_b A_b^{-1} C_b u_b^e = B_b u_b^e \tag{41}$$

u_b^e represents the nodal displacement vector for bending part,

$$u_b^e = \begin{Bmatrix} w_1 & \phi_{x1} & \phi_{y1} & \cdots & w_4 & \phi_{x4} & \phi_{y4} \end{Bmatrix} \tag{42}$$

The bending part stiffness can be attained.

$$K_b = \iint_{\Omega} B_b^T D_b B_b dxdy = C_b^T A_b^{-T} \iint_{\Omega} Q_b^T D_b Q_b^T dxdy A_b^{-1} C_b \tag{43}$$

$$D_b = \frac{Eh^3}{12(1-v^2)} \begin{bmatrix} 1 & v & 0 \\ v & 1 & 0 \\ 0 & 0 & \frac{1-v}{2} \end{bmatrix} \tag{44}$$

3.1.3 Shear part

In shell structures, especially in moderate thick shells, the transverse shear strains are secondary strains. According to the linear shell theory, shear strains are set to be const within the element domain. Accordingly we choose constant ϕ_x and ϕ_y and linear displacement field w. Because of the simplicity, matrix notation is not applied for displacement fields.

$$\begin{aligned} w &= e_0 + e_1 x + e_2 y \\ \phi_x &= f_0 \\ \phi_y &= f_1 \end{aligned} \tag{45}$$

$$\varepsilon_s = \begin{Bmatrix} \frac{\partial w}{\partial x} + \phi_y \\ \frac{\partial w}{\partial y} - \phi_x \end{Bmatrix} = \begin{Bmatrix} e_1 + f \\ e_2 - f \end{Bmatrix} = \begin{bmatrix} 1 & 0 \\ 0 & 1 \end{bmatrix} \begin{Bmatrix} h_1 \\ j_1 \end{Bmatrix} = Q_s a_s \tag{46}$$

The detailed formulation process is similar to the process of membrane and bending part and the process is omitted. Finally, the shearing strain can be expressed by the nodal displacement parameters, which is the same to that of the bending part. The stiffness matrix for the shear part is obtained.

$$K_s = \iint_\Omega B_s^T D_s B_s dxdy = C_s^T A_s^{-T} \iint_\Omega Q_s^T D_s Q_s^T dxdy A_s^{-1} C_s \tag{47}$$

$$D_s = \frac{5}{6} \frac{Eh}{2(1+v)} \begin{bmatrix} 1 & 0 \\ 0 & 1 \end{bmatrix} \tag{48}$$

3.2 Element stiffness matrix combining

In Section 3.1, the stiffness matrixes are calculated in membrane part, bending part and shear part separately. In this section the stiffness matrixes will be combined together according to the nodal freedom to form the complete element stiffness matrix. The complete nodal displacement vector is

$$u^e = \begin{Bmatrix} u_1 & v_1 & w_1 & \phi_{x1} & \phi_{y1} & \phi_{z1} & \cdots & u_4 & v_4 & w_4 & \phi_{x4} & \phi_{y4} & \phi_{z4} \end{Bmatrix} \tag{49}$$

The complete stiffness matrix is

$$K = K_m \oplus K_b \oplus K_s \tag{50}$$

In the above formulation, the$\oplus$notation represents construction according to the nodal freedoms, rather than the matrix adding. After the combination, the element stiffness matrix is calculated.

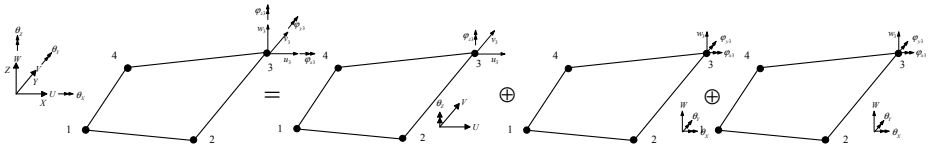

Figure 4: The membrane part, the bending part and the shear part are combined together to form complete element stiffness matrix

3.3 A method to reduce calculation

In the formulation process of the bending stiffness and the membrane stiffness, inverse of the matrix A_m and the matrix A_b must be calculated, which are 10-rank matrixes. Direct calculation of the inverse matrixes will be time consuming, so here we introduce a method to avoid the process. We take membrane part stiffness matrix as an example. The bending part stiffness can be calculated accordingly.

First, the membrane strains are reorganized,

$$\begin{aligned} \varepsilon'_m &= \begin{bmatrix} \varepsilon_{m1} \\ \varepsilon_{m2} \end{bmatrix} \\ \varepsilon_{m1} &= \begin{Bmatrix} \frac{\partial u}{\partial x} & \frac{\partial v}{\partial y} \end{Bmatrix}^T \quad \varepsilon_{m2} = \begin{Bmatrix} \frac{\partial u}{\partial y} & \frac{\partial v}{\partial x} \end{Bmatrix}^T \end{aligned} \tag{51}$$

Substitute Eq. (15) into Eq. (51),

$$\varepsilon_{m1} = \begin{cases} \frac{\partial u}{\partial x} = a_1 + 2a_3x + a_4y \\ \frac{\partial v}{\partial y} = b_2 + b_4x + 2b_5y \end{cases} \quad ; \quad \varepsilon_{m2} = \begin{cases} \frac{\partial v}{\partial x} = b_1 + 2b_3x + b_4y \\ \frac{\partial u}{\partial y} = a_2 + a_4x + 2a_5y \end{cases} \tag{52}$$

Now we treat these two parts of strains just like real membrane strains. First we calculate the ε_{m1} part.

$$\varepsilon_{m1} = Q_{m1}a_{m1} \tag{53}$$

The weak form of Eq. (53) is

$$\iint_\Omega Q_{m1}^T Q_{m1} dxdy \cdot a_{m1} = \iint_\Omega Q_{m1}^T \varepsilon_{m1} dxdy \tag{54}$$

Similar to standard procedure, we obtain the strain function.

$$\varepsilon_{m1} = Q_{m1}a_{m1} = Q_{m1}A_{m1}^{-1}C_{m1}u_m^e = B_{m1}u_m^e \tag{55}$$

In the above equation

$$B_{m1} = Q_{m1}A_{m1}^{-1}C_{m1} \quad A_{m1} = \iint_{\Omega} Q_{m1}^T Q_{m1} dxdy \tag{56}$$

The matrix A_{m1} is

$$A_{m1} = \begin{bmatrix} A_{m1}^1 & [0] \\ [0] & A_{m1}^2 \end{bmatrix} \tag{57}$$

$$A_{m1}^1 = \iint_{\Omega} \begin{bmatrix} 1 & 2x & y \\ 2x & 4x^2 & 2xy \\ y & 2xy & y^2 \end{bmatrix} dxdy \quad A_{m1}^2 = \iint_{\Omega} \begin{bmatrix} 1 & x & 2y \\ x & x^2 & 2xy \\ 2y & 2xy & 4y^2 \end{bmatrix} dxdy \tag{58}$$

Note that the rank of A_{m1}^1 and A_{m1}^2 are three, so the inverse matrixes can be calculated easily. The stiffness matrix connecting with strain ε_{m1} is

$$K_{m1} = \iint_{\Omega} B_{m1}^T D_{m1} B_{m1} dxdy = C_{m1}^T A_{m1}^{-T} \iint_{\Omega} Q_{m1}^T D_{m1} Q_{m1} dxdy A_{m1}^{-1} C_{m1} \tag{59}$$

$$D_{m1} = \frac{Eh}{1-v^2} \begin{bmatrix} 1 & v \\ v & 1 \end{bmatrix} \tag{60}$$

Using similar procedures, we get the stiffness matrix for ε_{m2} part,

$$K_{m2} = \iint_{\Omega} B_{m2}^T D_{m2} B_{m2} dxdy = C_{m2}^T A_{m2}^{-T} \iint_{\Omega} Q_{m2}^T D_{m2} Q_{m2} dxdy A_{m2}^{-1} C_{m2} \tag{61}$$

$$D_{m2} = \frac{Eh}{(1-v^2)} \frac{1-v}{2} \begin{bmatrix} 1 & 1 \\ 1 & 1 \end{bmatrix} \tag{62}$$

It can be proved

$$B_m^T D_m B_m = B_{m1}^T D_{m1} B_{m1} + B_{m2}^T D_{m2} B_{m2} \tag{63}$$

So the final stiffness matrix of membrane part is

$$K_m = K_{m1} + K_{m2} \tag{64}$$

In the above equation notation "+" represents matrix adding operation.

3.4 Consistent load

Assuming that the displacement field is linear within the domain,

$$w = e_0 + e_1 x + e_2 y \tag{65}$$

$\frac{\partial w}{\partial x}, \frac{\partial w}{\partial y}$ are taken as the generalized strain. Through calculation, the displacement field w can be expressed by the nodal parameters.

$$w = W^e u^e \tag{66}$$

With above equation we can calculate consistent load.

$$\iint_\Omega qw dxdy = \iint_\Omega qW^e u^e dxdy = \left(\iint_\Omega qW^e dxdy \right) u^e \tag{67}$$

4 Evaluation of element strain fields

4.1 Membrane

Now we calculation matrix C_m in Eq. (27), the following integrations are concerned.

$$\begin{aligned}
&\iint_\Omega \frac{\partial u}{\partial x} dxdy = \oint_s u n_x ds \\
&\iint_\Omega \frac{\partial u}{\partial x} y dxdy = \oint_s u y n_x ds \\
&\iint_\Omega \frac{\partial u}{\partial x} x dxdy = \oint_s u x n_x ds - \iint_\Omega u dxdy
\end{aligned} \tag{68}$$

S represents boundary of the element. Integrations along the boundary are approximately evaluated with sufficient accuracy. The Allman type functions are chosen, so the drilling degree of freedom is under consideration [Kim, Lomboy and Voyiadjis (2003)]. Along element side l_{ij}, the functions are set to be

$$\begin{aligned}
\bar{u} &= \frac{1}{2}(1-\varepsilon) u_i + \frac{1}{2}(1+\varepsilon) u_j + \frac{1}{8}(y_j - y_i)\left(1-\varepsilon^2\right)(\phi_{tj} - \phi_{ti}) \\
\bar{v} &= \frac{1}{2}(1-\varepsilon) v_i + \frac{1}{2}(1+\varepsilon) v_j - \frac{1}{8}(x_j - x_i)\left(1-\varepsilon^2\right)(\phi_{tj} - \phi_{ti})
\end{aligned} \tag{69}$$

u_i, u_j, v_i and v_j are in-plane displacements of node I and J; x_i, x_j, y_i and y_j are the local coordinates of node I and J. ϕ_{ti} represents the drilling degree of freedom on node I. The ε is

$$\varepsilon = \frac{1}{l}(2s-l) \quad for \quad 0 \le s \le l, -1 \le \varepsilon \le 1 \tag{70}$$

There are domain integrations $\iint\limits_{\Omega} udxdy$ and $\iint\limits_{\Omega} vdxdy$ in the formula. The integrations can be integrated by isoparametric mapping method. Interpolation functions for domain displacement fields are chosen to be [Nguyen-Van, Mai-Duy and Tran-Cong (2009)],

$$\begin{bmatrix} u \\ v \end{bmatrix} = \sum_{i=1}^{4} N_i(\xi,\eta) \begin{bmatrix} u_i \\ v_i \end{bmatrix} + \frac{1}{8} \sum_{k=5}^{8} N_k(\xi,\eta)(\phi_{zj} - \phi_{zi}) \begin{bmatrix} y_{ij} \\ x_{ij} \end{bmatrix} \tag{71}$$

Where

$$x_{ij} = x_j - x_i \quad y_{ij} = y_j - y_i \tag{72}$$

$$N_i(\xi,\eta) = \frac{1}{4}(1+\xi_i\xi)(1+\eta_i\eta) \quad i = 1,2,3,4 \tag{73}$$

$$N_k(\xi,\eta) = \frac{1}{2}\left(1-\xi^2\right)(1+\eta_k\eta) \quad k = 5,7 \tag{74}$$

$$N_k(\xi,\eta) = \frac{1}{2}(1+\xi_k\xi)\left(1-\eta^2\right) \quad k = 6,8 \tag{75}$$

The triplets (k,i,j) are set as $(5,1,2)$, $(6,2,3)$, $(7,3,4)$ and $(8,4,1)$. The isoparametric mapping within present formulation is used for integrations, which is different from isoparametric FEM. The integrations $\iint\limits_{\Omega} udxdy$ and $\iint\limits_{\Omega} vdxdy$ can be calculated numerically by Gauss integration or analytically as below.

$$\begin{aligned} \begin{bmatrix} \iint\limits_{\Omega} udxdy \\ \iint\limits_{\Omega} vdxdy \end{bmatrix} &= \sum_{i=1}^{4} \iint\limits_{\Omega} N_i(\xi,\eta)\,dxdy \begin{bmatrix} u_i \\ v_i \end{bmatrix} + \tfrac{1}{8} \sum_{k=5}^{8} \iint\limits_{\Omega} N_k(\xi,\eta)\,dxdy\,(\phi_{zj} - \phi_{zi}) \begin{bmatrix} y_{ij} \\ x_{ij} \end{bmatrix} \\ &= \sum_{i=1}^{4} \int_{-1}^{1}\int_{-1}^{1} N_i(\xi,\eta)\,|J|\,d\xi d\eta \begin{bmatrix} u_i \\ v_i \end{bmatrix} + \tfrac{1}{8} \sum_{k=5}^{8} \int_{-1}^{1}\int_{-1}^{1} N_k(\xi,\eta)\,|J|\,d\xi d\eta\,(\phi_{zj} - \phi_{zi}) \begin{bmatrix} y_{ij} \\ x_{ij} \end{bmatrix} \end{aligned} \tag{76}$$

In the above formula $|J|$ represents the determination of Jacob matrix J. The symbols i,j,k,l denote the element node arranged in anticlockwise sequence.

$$J = \frac{1}{4} \begin{bmatrix} -(1-\eta) & (1-\eta) & (1+\eta) & -(1+\eta) \\ -(1-\xi) & -(1+\xi) & (1+\xi) & (1-\xi) \end{bmatrix} \begin{bmatrix} x_i & y_i \\ x_j & y_j \\ x_k & y_k \\ x_l & y_l \end{bmatrix} \tag{77}$$

4.2 Bending part

Now we calculate matrix C_b. The following integrations are concerned.

$$\begin{aligned}
&\iint_{\Omega} \frac{\partial \phi_x}{\partial x} dxdy = \oint_s \phi_x n_x ds \\
&\iint_{\Omega} \frac{\partial \phi_x}{\partial x} ydxdy = \oint_s \phi_x y n_x ds \\
&\iint_{\Omega} \frac{\partial \phi_x}{\partial x} xdxdy = \oint_s \phi_x x n_x ds - \iint_{\Omega} \phi_x dxdy
\end{aligned} \tag{78}$$

For boundary integration, the following transformation equations are needed.

$$\begin{Bmatrix} \phi_x \\ \phi_y \end{Bmatrix} = \begin{bmatrix} n_x & -n_y \\ n_y & n_x \end{bmatrix} \begin{Bmatrix} \phi_s \\ \phi_n \end{Bmatrix} \tag{79}$$

String net functions and domain interpolation functions are chosen according to [Shi and Voyiadjis (1991a)]. We need the transformation because ϕ_x and ϕ_y are rotations along the global coordinate axis, while in formulation, the string net functions, denoted by ϕ_s and ϕ_n, are rotation functions along the element boundary.

String net functions along the boundary are chosen as,

$$\begin{aligned}
\phi_s(\varepsilon) &= -\frac{3}{2l}\lambda\left(1-\varepsilon^2\right) w_i + \frac{1}{4}\left[2-2\varepsilon-3\lambda\left(1-\varepsilon^2\right)\right]\phi_{si} \\
&\quad + \frac{3}{2l}\lambda\left(1-\varepsilon^2\right) w_j + \frac{1}{4}\left[2+2\varepsilon-3\lambda\left(1-\varepsilon^2\right)\right]\phi_{sj} \\
\phi_n(\varepsilon) &= \frac{1}{2}(1-\varepsilon)\phi_{ni} + \frac{1}{2}(1+\varepsilon)\phi_{nj}
\end{aligned} \tag{80}$$

$$\lambda = \frac{1}{1+12\frac{D_{b11}}{D_{q11}L^2}} \quad D_{b11} = \frac{Eh^3}{12(1-v^2)} \quad D_{q11} = \frac{5Eh}{12(1+v)} \tag{81}$$

where ε is set as (70). L is the character length of the shell. When the shell becomes very thin, which means $(h/L)^2 \to 0$, accordingly in Eq. (81) $\lambda \to 1$ and Eq. (69) becomes the Hermite interpolation function. Domain integration is calculated as below.

$$\begin{aligned}
&\iint_{\Omega} \phi_x(w_i, \phi_{xi}, \phi_{yi})\, dxdy \approx \iint_{\Omega} \left[\lambda \frac{\partial w}{\partial x} + (1-\lambda)\,\phi_x(\phi_{xi})\right] dxdy \\
&= \lambda \oint_s w n_x ds + (1-\lambda) \iint_{\Omega} \phi_x(\phi_{xi})\, dxdy
\end{aligned} \tag{82}$$

The remaining integration $\iint\limits_{\Omega} \phi_x(\phi_{xi})\,dxdy$ is calculated similar to Eq. (76).

4.3 Shear part

To make sure the Kirchhoff condition holds for extremely thin shell, similar to Eq. (82), the following formulations are used [Shi and Voyiadjis (1991a)],

$$\iint\limits_{\Omega}\left(\frac{\partial w}{\partial x}+\phi_y\right)dxdy=(1-\lambda)\left[\oint\limits_{s} wn_x ds+\iint\limits_{\Omega}\phi_y(\phi_{yi})\,dxdy\right] \tag{83}$$

$$\iint\limits_{\Omega}\left(\frac{\partial w}{\partial y}-\phi_x\right)dxdy=(1-\lambda)\left[\oint\limits_{s} wn_y ds-\iint\limits_{\Omega}\phi_x(\phi_{xi})\,dxdy\right] \tag{84}$$

λ is set in Eq. (81). When the shell becomes very thin, the Kirchhoff condition will be satisfied. The string net function for displacement field w is

$$\begin{aligned} w=&\frac{1}{2}\left[1-\xi+\frac{\lambda}{2}\left(\xi^3-\xi\right)\right]w_i+\frac{1}{2}\left[1+\xi-\frac{\lambda}{2}\left(\xi^3-\xi\right)\right]w_j\\ &+\frac{1}{4}\left[1-\xi^2+\lambda\left(\xi^3-\xi\right)\right]\cdot\frac{l}{2}\phi_{ni}+\frac{1}{4}\left[-1+\xi^2+\lambda\left(\xi^3-\xi\right)\right]\cdot\frac{l}{2}\phi_{nj}\end{aligned} \tag{85}$$

5 Numerical examples

Numerical examples are presented to validate the accuracy and effectiveness of the present element, which is denoted by QCS1. The results of present element are compared with other famous and success shell elements.

5.1 Bending patch test for thin plates

The bending patch test for thin plates is a well-known benchmark to validate the plate and shell elements for transverse shear locking [Chen, Wang and Zhao (2009)]. In analysis of thin plates a good C_0 type shell should also be able to give reliable results. The geometry and mesh for the patch test is depicted in Fig. 5. The thickness of the plate is set to be $t = 0.1$.The material is linear, isotropic elastic with properties $\mathrm{E} = 210\times10^5$ and $v = 0.3$. The element converges provided that patch test is satisfied for all second rank polynomial solutions of displacements. Here we consider only the pure bending solutions.

We choose analytic deflection field for thin plate bending as

$$w(x,y)=0.001x^2-0.0003y^2 \tag{86}$$

The rotation fields can be calculated under the Kirchhoff-Love assumptions.

$$\phi_x = \frac{\partial w}{\partial y} = -0.0006y; \quad \phi_y = -\frac{\partial w}{\partial x} = -0.002x. \tag{87}$$

Two types of patch tests are involved according to Section 9.3-9.4 of [Zienkiewicz, Taylor and Zhu (2005)]. In the patch test of form B, the exact transverse displacements and rotations are prescribed in nodes 1-4 according to Tab. 2. Displacements at inner node 5-8 are calculated. In patch test of form C, the node 2 is fully restrained and the node 1 is restrained only in the rotational degree of freedom in the y direction. Nodal forces are applied to nodes 3 and 4 according to the values in Tab. 2 and the displacements of all nodes are calculated. The present element passes these two types of patch tests.

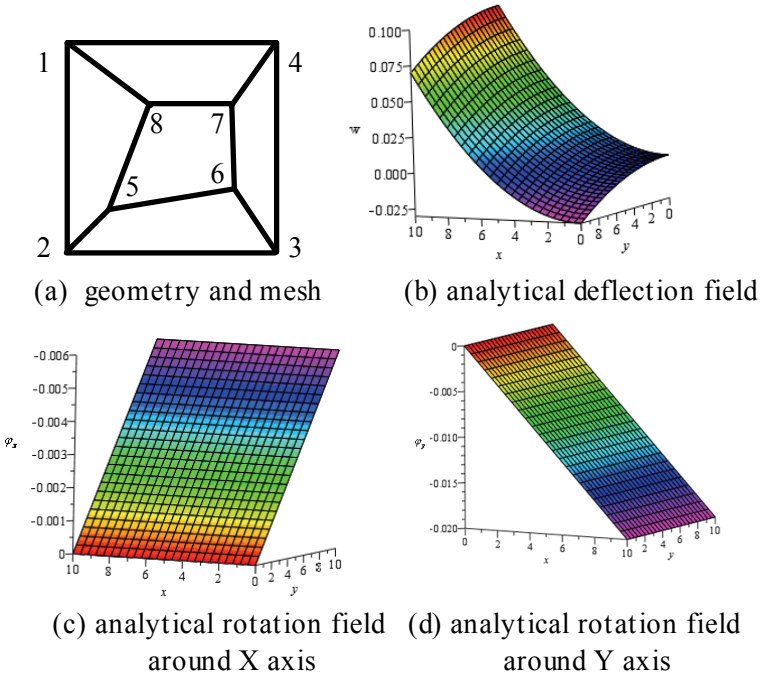

(a) geometry and mesh (b) analytical deflection field

(c) analytical rotation field around X axis (d) analytical rotation field around Y axis

Figure 5: Bending patch test of thin plate. The specified analytical displacement fields can be precisely represented by the present shell element.

Table 2: Coordinates of the nodes, the displacements and the forces of reaction for thin plate patch test

Node	X	Y	W	ϕ_x	ϕ_y	F_Z	F_{MX}	F_{MY}
1	0.0	10.0	-0.03	-0.006	0	0	17.5	0
2	0.0	0.0	0	0	0	0	17.5	0
3	10.0	0.0	0.1	0	-0.02	0	-17.5	0
4	10.0	10.0	0.07	-0.006	-0.02	0	-17.5	0
5	2.0	2.0	0.0028	-0.0012	-0.004	0.0	0.0	0.0
6	8.0	3.0	0.0613	-0.0018	-0.016	0.0	0.0	0.0
7	8.0	7.0	0.0493	-0.0042	-0.016	0.0	0.0	0.0
8	4.0	7.0	0.0013	-0.0042	-0.008	0.0	0.0	0.0

Table 3: Thin plate patch test results under different thickness/width ratio. "P" represents pass. The width equals to 10.

Thickness/width ratio	0.4	0.2	0.1	0.01	0.001	0.0001
Thickness	4	2	1	0.1	0.01	0.001
Patch test result	P	P	P	P	P	P

5.2 Mesh distortion sensitivity test: Razzaque's skew plate

This problem serves to test the mesh distortion sensitivity of the present element formulation. The geometry and boundary conditions are given in Fig. 6. Two opposite edges are simply supported and free on the other two edges. Plate span to thickness ratio $L/t = 1000$ ($L = 100$, $t = 0.1$). Material properties are Young's modulus $E = 1092000$ and Poisson's ratio $v = 0.3$. The loading is a uniformly distributed pressure of $q = 1$.

The central deflection and the central bending moments are obtained by the present element. Results are compared with those given by other researchers [Aksu Ozkul and Ture (2004); Soh, Cen, Long and Long (2001)] in Tab. 4, Tab. 5 and Fig. 7. The results prove that the present element is competitive compared with other elements and the bending moment results are especially good.

5.3 Shear locking test: clamped square plate

Square plate subjected to a concentrated load or a uniformly distributed load is modeled to evaluate the ability of elimination of shear locking. Clamped boundary on all four edges is applied. The symmetry condition is used and only a quarter of the plate is taken for analysis. Material properties are Young's modulus of E =

Table 4: Central deflection $w_c \cdot 100D/qL^4$ for Razzaque's skew plate

		[Aksu Ozkul and Ture (2004)]	[Soh, Cen, Long and Long (2001)]			
Mesh N×N	Present element	TURE12	ARS-Q12	MITC4	DKMQ	Reference
2×2	0.6903	0.6787	0.6666	0.3976	0.6666	0.7945
4×4	0.755367	0.7665	0.7691	0.6737	0.7695	
8×8	0.782457	0.7859	0.7876	0.7610	0.7876	
12×12	0.787293		0.7909	0.7785	0.7908	

Table 5: Central moment $M_y \cdot 1000/qL^2$ for Razzaque's skew plate

Mesh		[Aksu Ozkul and Ture (2004)]		[Soh, Cen, Long and Long (2001)]			
	Present element	TURE12	TURE24	MITC4	DKMQ	ARSQ12	Reference
2	95.4525	72.203	96.625	37.90	92.20	92.46	95.89
4	95.4893	89.453	97.375	77.60	96.00	95.95	
8	96.0982	94.358	96.297	90.90	96.10	96.05	
12	96.0541			93.70	96.00	96.02	

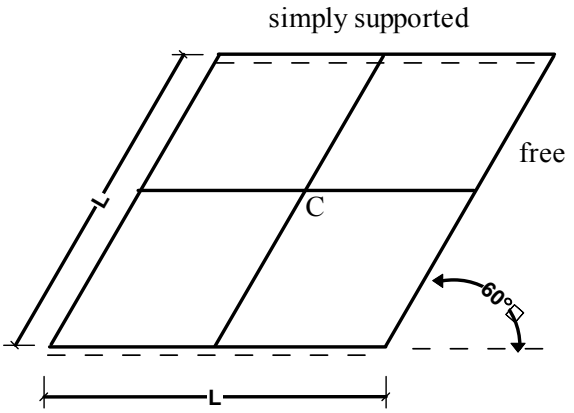

Figure 6: Razzaque's skew plate

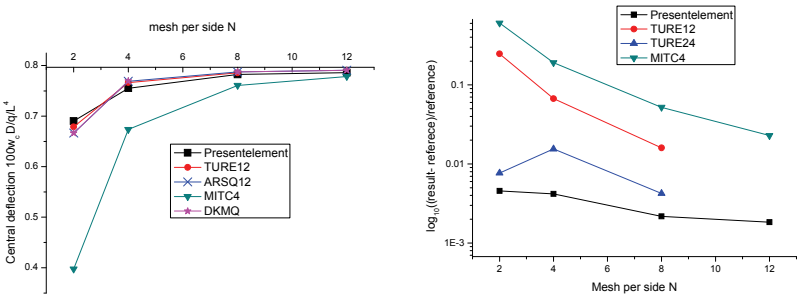

Figure 7: The convergence of the central deflection and central moment for Razzaque's skew plate

1.7472×10^7 and Poisson's ratio $v = 0.3$. The loading is $P = 10.0$ for concentrated load and $q = 1.0$ for uniformly distributed pressure. The geometry and computation models for square plate are shown in Fig. 8.

The results for clamped square plate under different loads compared with other researchers' results are listed in Tab. 6, Tab. 7 and Tab. 8 and Fig. 9 [Aksu Ozkul and Ture (2004)] , [Kim, Lomboy and Voyiadjis (2003)]. The length to thickness ratio ranges from 2.5 to 10000 and the result shows that present element do not have any shear locking problem. The result also proves that the present element has high precision and fast convergence.

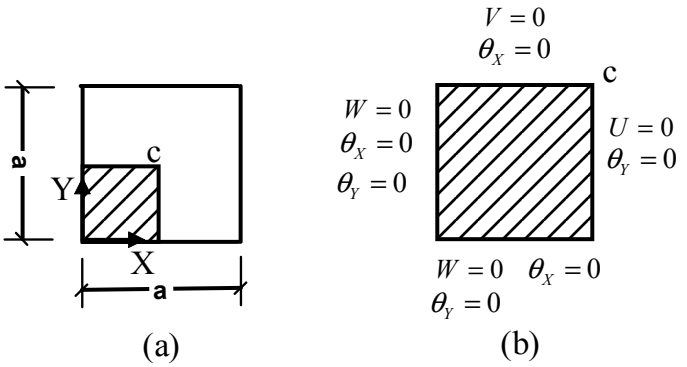

Figure 8: (a) Geometry model of square plate; (b) Computational model of clamped square plate.

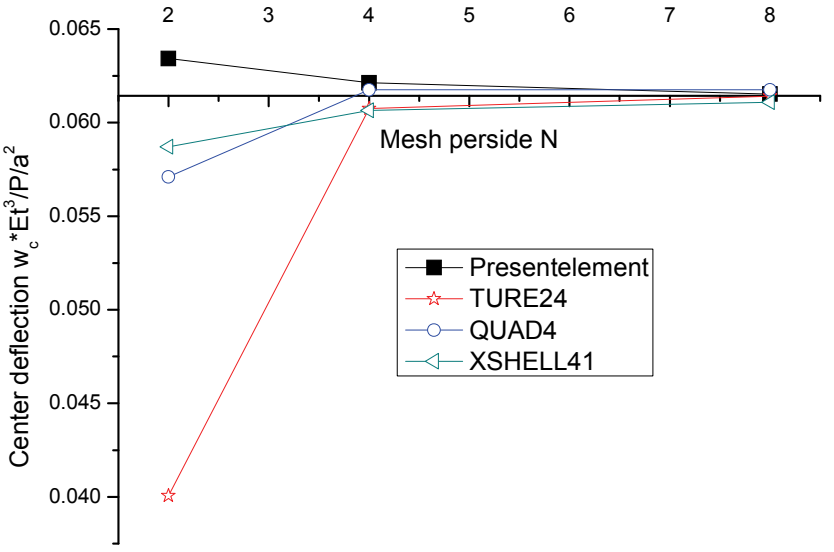

Figure 9: The convergence of the central deflection for clamped square plate under concentrated load

5.4 Bending moment test: simply supported square plate

Simply supported square plate subjected to a concentrated load is modeled to evaluate the bending moment results of the present element. The symmetry condition

Table 6: Central deflection $w_c \frac{Et^3}{pa^2}$ for clamped square plate under concentrated load P

Regular mesh		2×2	4×4	8×8	16×16
Present		0.06342	0.062128	0.06153	0.06135
TURE24	[Aksu Ozkul and Ture (2004)]	0.04006	0.06075	0.06141	
QUAD4	[Kim, Lomboy and Voyiadjis (2003)]	0.05711	0.06176	0.06176	
XSHELL41		0.05871	0.06066	0.0611	
Thin plate solution	[Aksu Ozkul and Ture (2004)]	0.0611			

Table 7: Central deflection $w_c \frac{Et^3}{pa^2}$ within different thickness/width ratio for clamped square plate under concentrated load with regular mesh 8×8

thickness/width	0.4	0.2	0.1	0.01	0.001	0.0001
thickness	0.8	0.4	0.2	0.02	0.002	0.0002
Present element	0.06496	0.06223	0.06169	0.06153	0.06153	0.06153
Thin plate result	0.0611					

Table 8: Central moments $100M_x/\left(qa^2\right)$ for clamped square plate under uniform load q with 8×8 mesh; plate span is set to be 2.

Thickness span ratio	5	10	100	1000
Thickness	0.4	0.2	0.02	0.002
Present element	2.32523	2.3223	2.321265	2.321255
Thin plate solution	2.31			

is used and only a quarter of the plate is taken for analysis. Material properties are Young's modulus of E $= 1.7472 \times 10^7$ and Poisson's ratio $v = 0.3$. The loading is $P = 10.0$.The geometry and computation models are shown in Fig. 10.

The bending moment along the central axis line is calculated. The analytical bending result [Timoshenko, Stephen and Woinawsky (1959)] is given by Eq. (88). In the equation $\gamma_1 = -0.565$ and $\gamma_2 = 0.135$. Symbol r represents the distance between concerned point and the center of plate c and symbol a represents the square

span.

$$M_x = \frac{P(1+\nu)}{4\pi}\left(\ln\left(\frac{2a}{\pi r}\right)\right) + \gamma_1 \frac{P}{4\pi} \quad M_y = \frac{P(1+\nu)}{4\pi}\left(\ln\left(\frac{2a}{\pi r}\right)\right) + \gamma_2 \frac{P}{4\pi} \tag{88}$$

Substitute all the parameters into above equation and we get

$$M_x = -0.91678 - 1.0345\ln\left(\frac{r}{a}\right) \quad M_y = -0.359736 - 1.0345\ln\left(\frac{r}{a}\right) \tag{89}$$

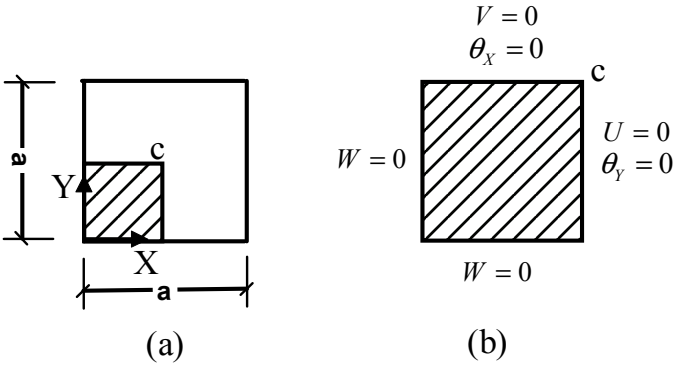

Figure 10: (a) Geometry model of square plate; (b) Computational model of simply supported plate.

Results calculated by present element are listed in Fig. 11. From the results we can conclude that the present element has high precision for bending moment, especially for area near the plate center, where the bending moment is of most importance. The results for areas near the boundary are slightly away from the analytical solution, while the bending moments there are near zero and are less important.

5.5 Membrane locking test: Pinched cylinder with rigid diaphragms

The pinched cylinder problem is considered to be one of the most demanding benchmark problems in shell analysis. This test is severe for the in-extensible bending and complex membrane stress state. The geometric and computational models are given in Fig. 12. The symmetry conditions are applied to reduce the calculation. The cylinder's radius $R = 300.0$, Length $L = 600.0$, thickness $t = 3.0$. The material properties are: Young's modulus $\mathrm{E} = 3.0 \times 10^6$ and Poisson's ratio $\nu = 0.3$. The concentrated load $P = 1.0$. The deflection of the point under load is calculated. Results are listed in Tab. 9 and Fig. 13 [Choi and Lee (2003); Kim, Lomboy and Voyiadjis (2003)]. The results show present element is free from membrane locking.

Table 9: The deflection of the point under load of pinched cylinder

	Present element		XSHELL42		MITC4		Type-I [Choi and Lee (2003)]		Reference result 1×10^{-5}
Mesh	Result 1×10^{-5}	Relative error %	Result 1×10^{-5}	Relative error %	Result 1×10^{-5}	Relative error %	Result 1×10^{-5}	Relative error %	1.8248
4×4	1.11135	39.10	1.1405	37.5	0.6752	62.9987	0.7	61.6	
8×8	1.68894	7.445	1.6752	8.1981	1.3504	25.9974	1.37	25	
16×16	1.84879	1.3147	1.8102	0.8	1.6971	6.9980	1.699	6.9	

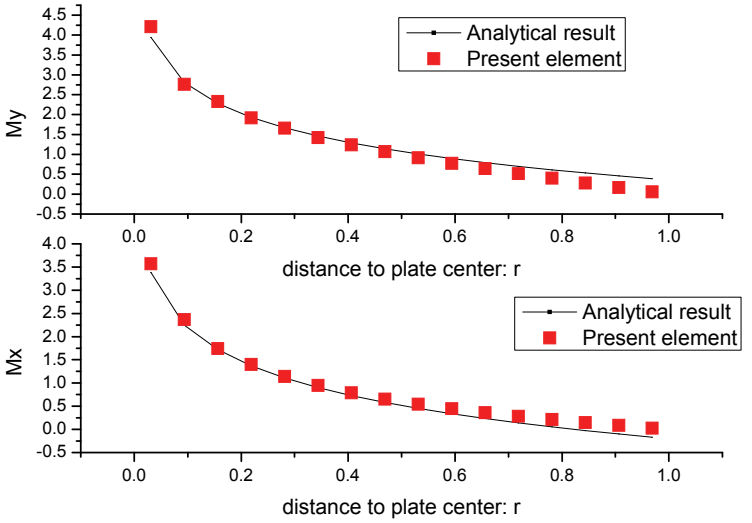

Figure 11: Bending moment M_X and M_Y along central axis $Y = 1$ of plate

5.6 *Comparison with assumed strain quasi-conforming shell: Morley's skew plate*

We choose XSHELL element of K.D. Kim et al. [Kim, Lomboy and Voyiadjis (2003)] as a representation of the assumed strain QC shell. The XSHELL element is a plat shell element with six degrees of freedom per node and has similar string functions to present element, so it is suitable for comparison. Morley's skew plate problem is chosen because this is the only test available with both displacement and bending moment results obtained by XSHELL. The geometry and boundary conditions are given in Fig. 14. All four edges are simply supported. The thickness is $10mm$ and side length is $L = 1000$mm. Material properties are Young's modulus of $E = 30N/mm^2$ and Poisson's ratio$v = 0.3$. The loading is a uniformly distributed pressure $q = 1.0 \times 10^{-6} N/mm^2$. The full plate is used in the model.

The analytical solutions given by [Morley (1963)] are $w_c \cdot 1000D/\left(ql^4\right) = 0.408$, bending moment $M_{\max} \cdot 100/\left(ql^2\right) = 1.910$ and $M_{\min} \cdot 100/\left(ql^2\right) = 1.080$. Results of elements ARS-Q12 and Q4BL from [Soh, Cen, Long and Long (2001)] are listed along for compare. The results of deflection of central point C are listed in Tab. 10. The maximum and minimum bending moments are listed in Tab. 11. In Fig. 15, the results show that present element is competitive compared with XSHELL and

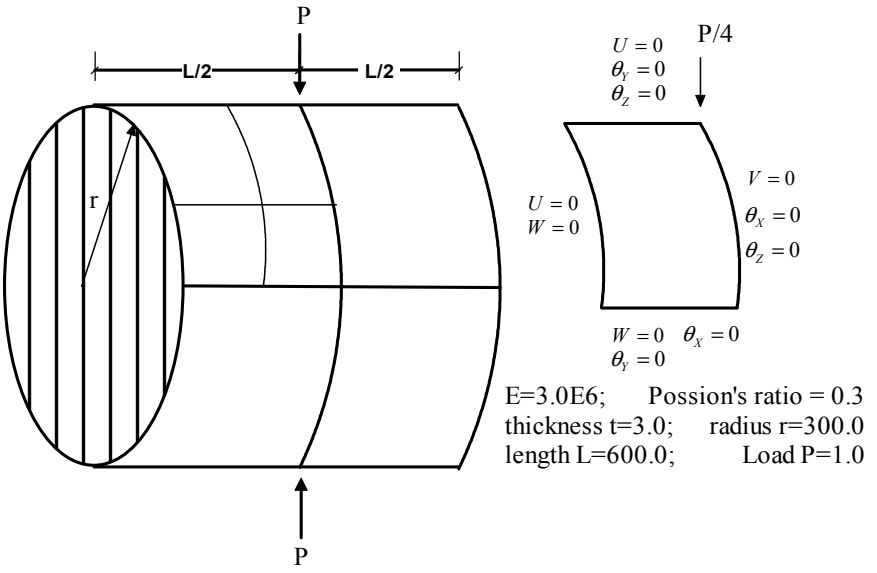

Figure 12: Pinched cylinder problem

has more stable performance.

Table 10: Deflection $w_c \cdot 1000D/\left(ql^4\right)$ of central point C

Mesh	4×4	8×8	14×14	32×32
Present element	0.4792	0.4244	0.4216	0.4183
XSHELL	0.4346	0.4203	0.4195	
ARS-Q12	0.7535	0.5033		0.4230
Q4BL	0.513381	0.440180		0.426951
analytical	0.4080			

6 Results

An assumed displacement QC finite element method is introduced to direct the development of the QC elements. In the framework, the formulation starts from truncated polynomial expansion of displacements; the expansion of the strains are derived according to the displacement-strain relationship. In the present method, a four node quadrilateral flat shell element with excellent strain/stress results and stable convergence rate is developed. The element possesses a complete linear mem-

Table 11: Results of maximum moments $M_{\max} \cdot 100/\left(ql^2\right)$ and minimum moments $M_{\min} \cdot 100/\left(ql^2\right)$ in central point C

Mesh	Present element	XSHELL	ARS-Q12	Q4BL	Present element	XSHELL	ARS-Q12	Q4BL
	$M_{\max} \cdot 100/\left(ql^2\right)$				$M_{\min} \cdot 100/\left(ql^2\right)$			
4	2.33585	2.44289	2.30990	2.014126	1.50328	1.44936	1.72320	1.131812
8	2.01161	1.87753	2.06697	1.991977	1.28476	1.17936	1.26733	1.164247
14	1.93991	1.94438			1.13958	1.11780		
32	1.93885		1.94729	1.961831	1.13361		1.13681	1.148773
analytical	1.91000				1.08000			

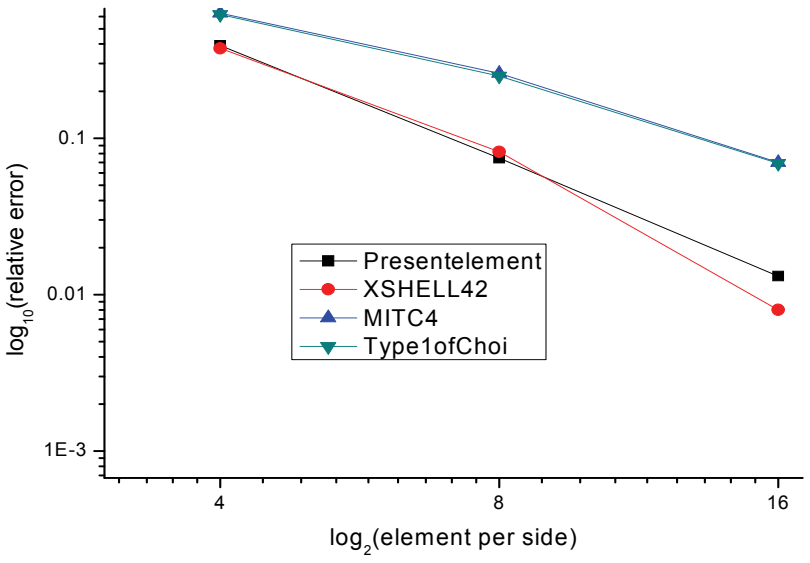

Figure 13: The convergence of deflection in the point under load

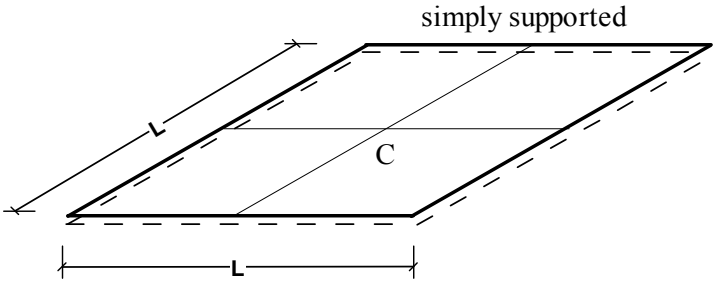

Figure 14: Morley's skew plate

brane and bending fields of strain, free from any incomplete high order items. The consistent nodal force is easily calculated in the present formulation. Advantages of QC are preserved, and the present shell element has an explicit stiffness matrix and convenient post-processing; additionally it is free from membrane locking and shear locking.

The assumed displacement complements QC by appending in-domain displacement fields. Researchers who are familiar with the conventional finite element

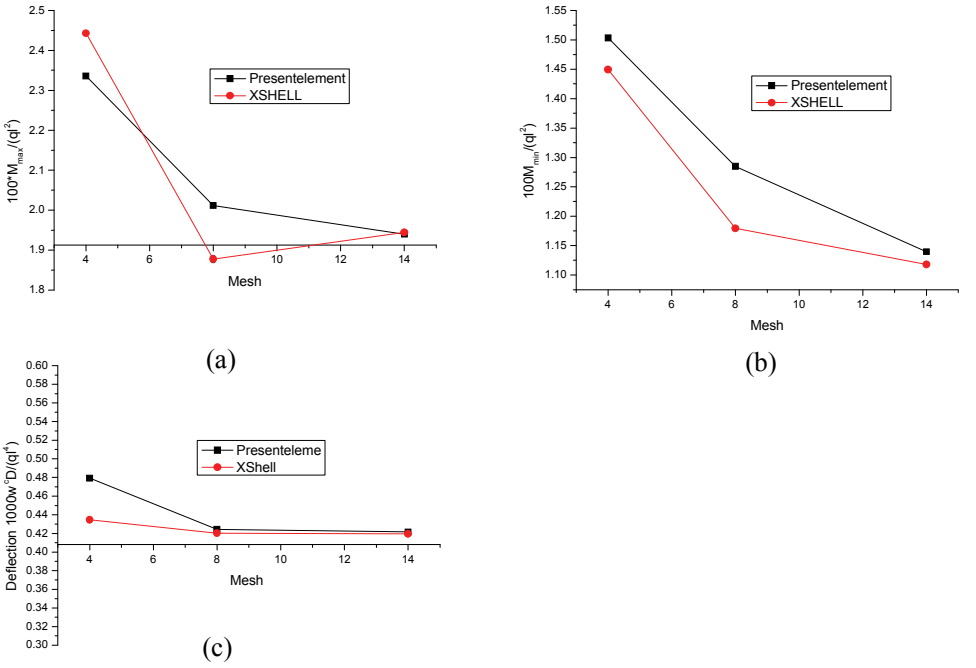

Figure 15: Compare between present element and XSHELL: (a) maximum moments $M_{\max} \cdot 100/\left(ql^2\right)$; (b) minimum moments $M_{\min} \cdot 100/\left(ql^2\right)$; (c) deflection $w_c \cdot 1000D/\left(ql^4\right)$.

method that is developed using interpolation displacement functions can easily understand the new frame. We believe the assumed displacement QC is more competent than the assumed strain one and better elements can be developed. The present shell element addresses linear problems and can be extended for nonlinear analysis.

Acknowledgement: This work was funded by the Key Project of the National Natural Science Foundation of China (No. 10932003), "863" Project of China (No. 2009AA04Z101), and "973" National Basic Research Project of China (No. 2010CB832700). These supports are gratefully acknowledged. Many thanks are due to the referees for their valuable comments. The second author is grateful to the editorial support from Doctor Candidate JingKai Wu and Doctor Candidate ShiYi Liu.

7 References

Aksu Ozkul, T.; Ture, U. (2004): The transition from thin plates to moderately thick plates by using finite element analysis and the shear locking problem, *Thin-Walled Structures*, vol. 42, no. 10, pp. 1405-1430.

Cai, Y. C.; Paik, J. K.; Atluri, S. N. (2010): A Triangular Plate Element with Drilling Degrees of Freedom, for Large Rotation Analyses of Built-up Plate/Shell Structures, Based on the Reissner Variational Principle and the von Karman Nonlinear Theory in the Co-rotational Reference Frame, *CMES: Computer Modeling in Engineering & Sciences*, vol. 61, no. 3, pp. 273-312.

Chen, W.; Wang, J.; Zhao, J. (2009): Functions for patch test in finite element analysis of the Mindlin plate and the thin cylindrical shell, *Science in China Series G: Physics Mechanics and Astronomy*, vol. 52, no. 5, pp. 762-767.

Choi, C. K.; Lee, T. Y. (2003): Efficient remedy for membrane locking of 4-node flat shell elements by non-conforming modes, *Computer Methods in Applied Mechanics and Engineering*, vol. 192, no. 16-18, pp. 1961-1971.

He, D. S.; Tang, L. M. (2002): The displacement function of quasi-conforming element and its node error, *Applied Mathematics and Mechanics-English Edition*, vol. 23, no. 2, pp. 127-137.

Kim, K. D.; Lomboy, G. R.; Voyiadjis, G. Z. (2003): A 4-node assumed strain quasi-conforming shell element with 6 degrees of freedom, *International Journal for Numerical Methods in Engineering*, vol. 58, no. 14, pp. 2177-2200.

Lomboy, G. R.; Suthasupradit, S.; Kim, K. D.; Onate, E. (2009): Nonlinear Formulations of a Four-Node Quasi-Conforming Shell Element, *Archives of Computational Methods in Engineering*, vol. 16, no. 2, pp. 189-250.

Lu, H. X.; Xu, S. N. (1989): An effective quadrilateral plate bending element, *International Journal for Numerical Methods in Engineering*, vol. 28, no. 5, pp. 1145-1160.

Morley, L. S. D. (1963): *Skew plates and structures*, 2nd edition, Oxford, Pergamon Press.

Nguyen-Van, H.; Mai-Duy, N.; Tran-Cong, T. (2009): An Improved Quadrilateral Flat Element with Drilling Degrees of Freedom for Shell Structural Analysis, *CMES: Computer Modeling in Engineering & Sciences*, vol. 49, no. 2, pp. 81-111.

Shi, G.; Voyiadjis, G. Z. (1991a): Efficient and accurate four-node quadrilateral plate bending element based on assumed strain fields, *International Journal for Numerical Methods in Engineering*, vol. 32, no. 5, pp. 1041-1055.

Shi, G.; Voyiadjis, G. Z. (1991b): Geometrically nonlinear analysis of plates by assumed strain element with explicit tangent stiffness matrix, *Computers & Struc-*

tures, vol. 41, no. 4, pp. 757-763.

Shi, G.; Voyiadjis, G. Z. (1993): A computational model for FE ductile plastic damage analysis of plate bending, *Journal of Applied Mechanics*, vol. 60, no. 3, pp. 749-758.

Soh, A. K.; Cen, S.; Long, Y. Q.; Long, Z. F. (2001): A new twelve DOF quadrilateral element for analysis of thick and thin plates, *European Journal of Mechanics-A/Solids*, vol. 20, no. 2, pp. 299-326.

Tang, L.; Liu, Y. (1985): Quasi-conforming element techniques for penalty finite element methods, *Finite Elements in Analysis and Design*, vol. 1, no. 1, pp. 25-33.

Tang, L. M.; Chen, W. J.; Liu, Y. X. (1980): Quasi-conforming elements for finite element analysis, *J Dalian Inst Technol*, vol. 10, no. 2, pp. 17-35.

Tang, L. M.; Liu, Y. X. (1984): Quasi-Conforming element techniques for penalty finite element methods, *Finite Elements in Analysis and Design*, vol. 1, no. 1, pp. 25-33.

Timoshenko, S.; Stephen, P.; Woinawsky, K. S. (1959): *Theory of plates and shells*, 2nd edition, McGraw Hill Book Company.

Yang, H. T. Y.; Saigal, S.; Masud, A.; Kapania, R. K. (2000): A survey of recent shell finite elements, *International Journal for Numerical Methods in Engineering*, vol. 47, no. 1-3, pp. 101-127.

Zienkiewicz, O. C.; Taylor, R. L.; Zhu, J. Z. (2005): *The finite element method: its basis and fundamentals*, 6th edition, Elsevier Butterworth-Heinemann.